Characterization and catalytic properties of combustion synthesized Au/CeO_2 catalyst

Parthasarathi Bera and M.S. Hegde *

Solid State and Structural Chemistry Unit, Indian Institute of Science, Bangalore 560012, India

Received 14 August 2001; accepted 4 December 2001

Ceria-supported Au catalyst has been synthesized by the solution combustion method for the first time and characterized by X-ray diffraction (XRD), transmission electron microscopy (TEM) and X-ray photoelectron spectroscopy (XPS). Au is dispersed as Au^0 as well as Au^{3+} states on CeO_2 surface of 20–30 nm crystallites. On heating the as-prepared 1% Au/CeO_2 in air, the concentration of Au^{3+} ions on CeO_2 increases at the expense of Au^0. Catalytic activities for CO and hydrocarbon oxidation and NO reduction over the as-prepared and the heat-treated 1% Au/CeO_2 have been carried out using a temperature-programmed reaction technique in a packed bed tubular reactor. The results are compared with nano-sized Au metal particles dispersed on α-Al_2O_3 substrate prepared by the same method. All the reactions over heat-treated Au/CeO_2 occur at lower temperature in comparison with the as-prepared Au/CeO_2 and Au/Al_2O_3. The rate of NO + CO reaction over as-prepared and heat-treated 1% Au/CeO_2 are 28.3 and 54.0 μmol g^{-1} s^{-1} at 250 and 300 °C respectively. Activation energy (E_a) values are 106 and 90 kJ mol^{-1} for $CO + O_2$ reaction respectively over as-prepared and heat-treated 1% Au/CeO_2 respectively.

KEY WORDS: combustion synthesis; Au/CeO_2; NO; CO; hydrocarbon; reduction; oxidation.

1. Introduction

Bulk gold has been regarded to be a catalytically inactive metal due to its $5d^{10}$ configuration. Recent studies have shown that small gold particles dispersed on different oxide supports such as Fe_2O_3, MnO_2, Co_3O_4, NiO, CuO, ZnO, TiO_2 SiO_2, ZrO_2 and Al_2O_3 are active for low temperature CO oxidation [1–12]. Gold catalysts are now being studied intensively also for low temperature hydrogenation, water–gas shift reaction, hydrocarbon oxidation and NO reduction [13–22]. However, preparation conditions, size of gold particles, catalyst pretreatment and presence of suitable metal oxide substrates play an important role for high activity of supported gold catalysts [23–28]. Further, the exact nature of active species is not yet fully understood. It has been suggested that the catalytic activity is attributed to the presence of ionic Au species or metallic Au. Recent studies predict that Au^+ species are more active than Au^0 [29,30].

Generally gold is dispersed on oxide supports by conventional methods such as impregnation, deposition–precipitation or co-precipitation. However, relatively little study exists in the literature on CeO_2 supported Au catalyst [18,31,32]. Shaw *et al.* [31] have shown CO hydrogenation over Au/CeO_2 catalyst. Liu and Flytzani-Stephanopoulos [32] have reported oxidation of CO and CH_4 over Au/CeO_2 catalyst prepared by the co-precipitation method. Recently, our group has reported the synthesis of CeO_2 and Al_2O_3 supported Cu, Pt, Pd and Ag catalysts by the combustion method and their catalytic activities towards NO reduction, CO and hydrocarbon oxidation [33–36]. Here we report the dispersion of Au on CeO_2 support by the combustion technique where Au is present in the Au^0 as well as the Au^{3+} state. Thermally treated Au/CeO_2 shows an increase in Au^{3+} ion concentration on CeO_2 and higher catalytic activities toward NO reduction, CO and hydrocarbon oxidation in relation to as-prepared Au/CeO_2. On the other hand, fine Au particles dispersed on Al_2O_3 support by the same method [34] shows the lowest catalytic activity.

2. Experimental

2.1. Synthesis

The combustion mixture for the preparation of 1% Au/CeO_2 contained $(NH_4)_2Ce(NO_3)_6$, $HAuCl_4$ (Ranbaxy Laboratories, Ltd., 99%) and $C_2H_6N_4O_2$ (oxalyldihydrazide) in the mole ratio of 0.99 : 0.01 : 2.376. Oxalyldihydrazide (ODH) was used as the fuel. In a typical preparation, 10 g of $(NH_4)_2Ce(NO_3)_6$ (E. Merck India Ltd., 99%), 0.063 g of $HAuCl_4$ (E. Merck India Ltd., 99.9%) and 5.175 g of ODH were dissolved in the minimum volume of water in a borosilicate dish of 130 cm^3 capacity. The dish containing the redox mixture was introduced into a muffle furnace maintained at

* To whom correspondence should be addressed.
E-mail: mshegde@sscu.iisc.ernet.in, partho@sscu.iisc.ernet.in

1011-372X/02/0400-0075/0

350 °C. The solution boiled with frothing and foaming, and ignited to burn with a flame (~1000 °C) yielding a voluminous solid product within 5 min. 1% Au/CeO_2 sample is light violet in color. Similarly, 2% Au/CeO_2 was also prepared by this method. Details of the preparation of Au/Al_2O_3 have been described elsewhere [34]. As-prepared 1% Au/CeO_2 was heated at 800 °C for 100 h in air and the color of the sample changed from light violet to light gray.

2.2. Characterization

XRD patterns of Au/CeO_2 were recorded on a JEOL JDX-8P diffractometer using Cu K_α radiation with a scan rate of $2^\circ\,min^{-1}$. TEM studies of as-prepared as well as heat-treated Au/CeO_2 powders were carried out using a JEOL JEM-200CX electron microscope operated at 200 kV.

XPS of the supported Au catalyst were recorded on an ESCA-3 Mark II spectrometer (VG Scientific Ltd., England) using Al K_α radiation (1486.6 eV). Binding energies were calculated with respect to C(1s) at 285 eV. For XPS analysis the powder samples were made into pellets of 8 mm diameter and placed into an ultra high vacuum (UHV) chamber at 10^{-9} Torr housing the analyzer. Before mounting the sample in the analyzing chamber it was kept in the preparation chamber at 10^{-9} Torr for 5 h in order to desorb any volatile species present on the sample. The experimental data were curve fitted with Gaussian peaks after subtracting a linear background. The concentrations of different states were estimated from the area of the respective Gaussian peaks.

2.3. Temperature programmed reaction (TPR)

The gas–solid reactions were carried out in a home-made TPR system equipped with a quadrupole mass spectrometer QXK300 (VG Scientific Ltd., England) using a packed bed tubular reactor. Typically, 0.1–0.2 g of the catalyst was taken in a quartz tube reactor of 20 cm length and 6 mm diameter which was heated from 30 to 750 °C at a rate of $15\,^\circ C\,min^{-1}$. The quartz tube was evacuated to 10^{-6} Torr. The gaseous products were sampled through a fine control leak valve to a UHV system housing the quadrupole mass spectrometer at 10^{-9} Torr. The gases were passed over the catalyst at a flow rate of $25\,\mu mol\,s^{-1}$ which can be varied from 10 to $40\,\mu mol\,s^{-1}$. Accordingly, the space velocity was in the range 5×10^{-5} to $2\times10^{-4}\,mol\,g^{-1}\,s^{-1}$. The dynamic pressure of gases was in the range 1–20 Torr in the reaction system in all the experiments. All the masses were scanned in every 10 s. The intensity of each mass as a function of temperature (thermogram) was generated at the end of the reaction. The gases were obtained from Bhoruka Gases Ltd., Bangalore. Their purities were better than 99% as analyzed by the quadrupole mass spectrometer.

3. Results

3.1. Structrual studies

The XRD patterns of as-prepared 1% Au/CeO_2 show that the diffraction lines can be indexed to the fluorite structure and the d values agree well with those for CeO_2. In addition to diffraction lines due to CeO_2, a very weak peak of Au metal is observed in the XRD pattern. The crystallite sizes of CeO_2 calculated from Debye–Scherrer method are in the range 20–35 nm. The XRD pattern of heat-treated Au/CeO_2 did show an Au(111) peak but with less intensity. Relative intensity of Au(111) to CeO_2(111) is 1.8% in the as-prepared sample against 1% in the heated sample. Au/CeO_2 prepared by co-precipitation, however, shows intense Au metal peaks in XRD patterns [32]. Therefore, decrease in Au(111) peaks suggests that part of Au in the as-prepared sample might have reacted with the CeO_2 matrix.

TEM of 1% Au/CeO_2 shows that the average size of CeO_2 crystallites is 30 nm. Small gold metal particles could be observed on the CeO_2 crystallite surface. The particle sizes of Au calculated from TEM are 5–10 nm. The electron diffraction ring pattern could be indexed to polycrystalline CeO_2 in a fluorite structure along with the Au(111) metal ring. The morphology of CeO_2 crystallites is cubic. TEM of thermally treated Au/CeO_2 does not distinguish Au particles as seen in the as-prepared sample. There is increase in average crystallite size of CeO_2 from 30 to 40 nm due to heat treatment. Further, a distinct Au(111) ring is not observed in the electron diffraction pattern of the heat-treated sample. Bright field images of as-prepared and heat-treated samples are given in figure 1.

3.2. XPS studies

XPS of Au(4f) in 1% Au/CeO_2 shows the peaks due to multiple oxidation states. Typical XPS of the core level region of Au(4f) in as-prepared and heat-treated 1% Au/CeO_2 are shown in figure 2. The Au(4f) spectrum for Au/Al_2O_3 is also shown in figure 2(c) for comparison. As seen from figure 2, the intensity of Au($4f_{5/2}$) envelope is higher than the Au($4f_{7/2}$) in Au/CeO_2. This clearly indicates that Au is in multiple oxidation states. Accordingly, Au(4f) peaks in Au/CeO_2 could be deconvoluted into sets of spin–orbit doublets and Au($4f_{7/2,5/2}$) peaks at 84.0, 87.9 eV and 87.1, 90.8 eV correspond to Au^0 and Au^{3+} oxidation states. Relative intensities of Au^0 and Au^{3+} are 70 and 30% respectively in as-prepared 1% Au/CeO_2 (figure 2(a)). However, Au($4f_{7/2,5/2}$) peaks are observed at 84.0, 87.8 eV and 86.6, 90.3 eV in the heat treated sample. The shifted Au(4f) peaks could be assigned to the Au^{3+} state [1,37] and relative intensities of Au^0 and Au^{3+} are 57 and 43% respectively. On heating, increase in total Au(4f) as well as particular

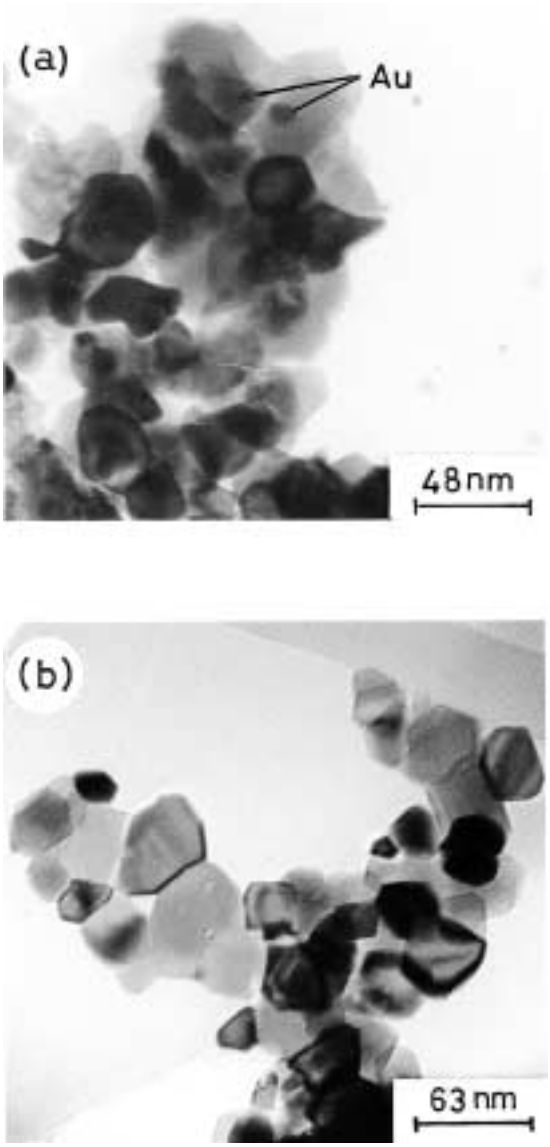

Figure 1. TEM of (a) as-prepared and (b) heat-treated 1% Au/CeO_2.

Au^{3+} intensities is observed. In 1% Au/Al_2O_3, Au is present only in the Au^0 state, as can be seen from figure 2(c). Thus, in the combustion synthesized 1% Au/CeO_2, Au is present in metallic as well as +3 oxidation states. In figure 3, Ce(3d) spectra obtained from as-prepared and heat-treated 1% Au/CeO_2 are given. The spectra with satellite features (marked in the figure) correspond to Ce^{4+} in CeO_2 [38]. No significant variation in the Ce(3d) spectrum is seen in the heat-treated sample, indicating that Ce is present in the +4 state after heat-treatment. XPS of 1% Au/CeO_2 catalyst after $CO + O_2$ and $CH_4 + O_2$ reactions was also carried out. There is no noticeable change in the XPS of Au(4f) and Ce(3d) core level regions in the spent catalyst.

The surface concentration of Au in 1% Au/CeO_2 has been estimated by the relation:

$$\frac{X_{Au}}{X_{Ce}} = \frac{I_{Au}}{I_{Ce}} \frac{\sigma_{Ce}\lambda_{Ce}D_E(Ce)}{\sigma_{Au}\lambda_{Au}D_E(Au)} \quad (1)$$

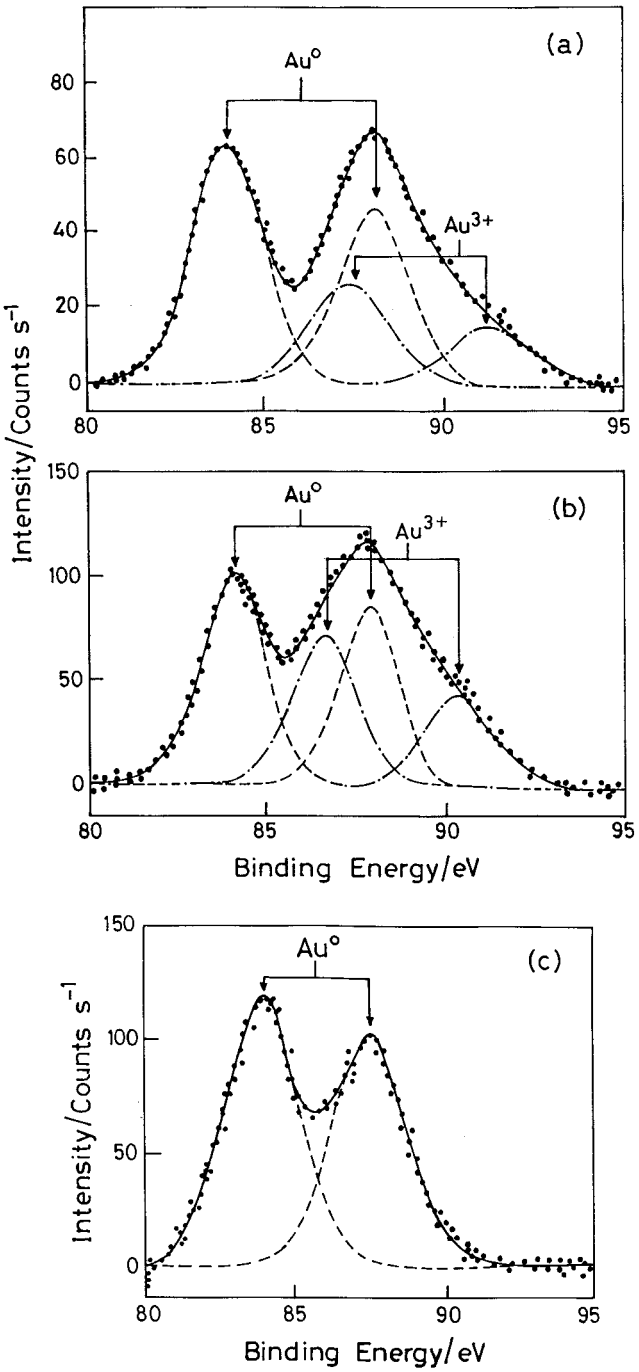

Figure 2. XPS of Au(4f) core level region in (a) as-prepared, (b) heat-treated 1% Au/CeO_2 and (c) 1% Au/Al_2O_3.

where X, I, σ, λ and D_E are the surface concentration, intensity, photoionization cross section, mean escape depth and geometric factor respectively. Integrated intensities of Au(4f) and Ce(3d) peaks have been taken into account to estimate the concentration. Photoionization cross sections and mean escape depths have been obtained from the literature [39,40]. Accordingly, surface concentrations of Au are 10 and 16% on as-prepared and heat-treated 1% Au/CeO_2 respectively. On the other hand, surface concentration of Au in 1% Au/Al_2O_3 is

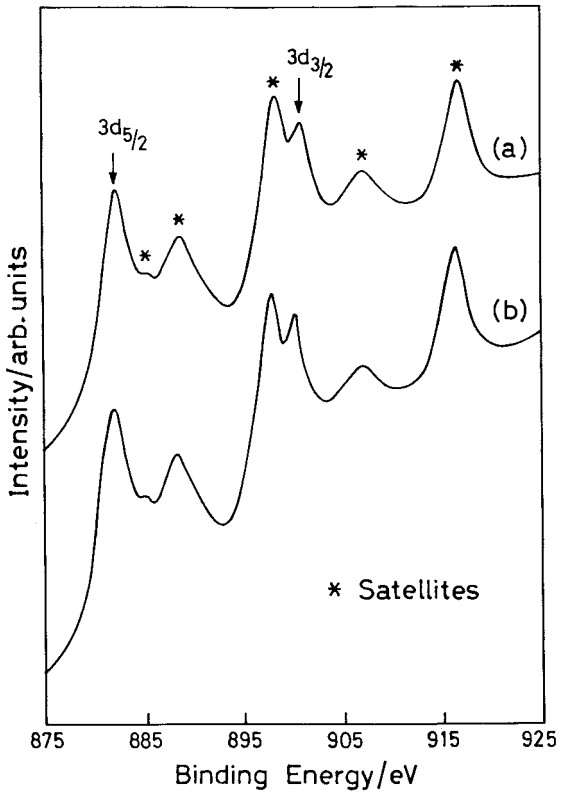

Figure 3. XPS of Ce(3d) core level region in as-prepared 1% Au/CeO_2.

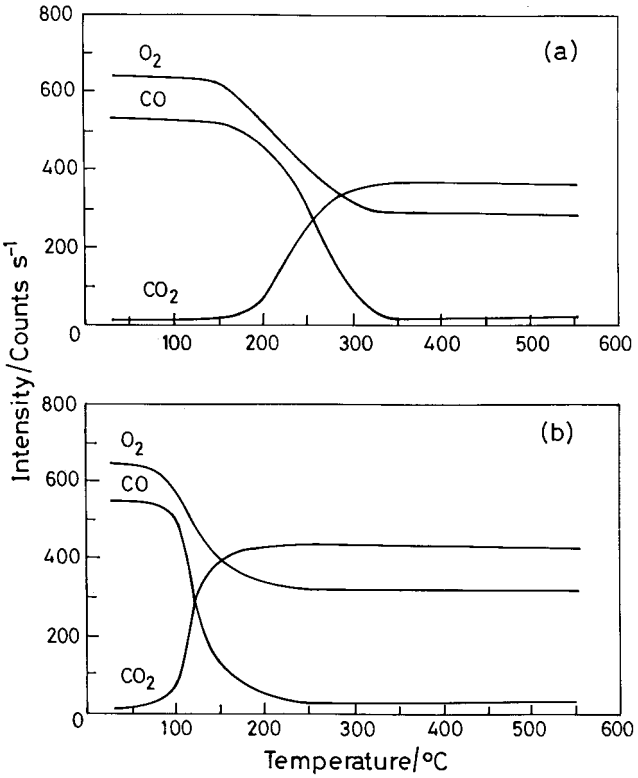

Figure 4. TPR profiles of $CO + O_2$ reactions over (a) as-prepared and (b) heat-treated 1% Au/CeO_2.

0.8%, which is close to the bulk concentration of Au metal in 1% Au/Al_2O_3. Thus, higher dispersion of Au is achieved over CeO_2 support.

3.3. TPR studies

Catalytic properties of Au/CeO_2 towards NO reduction by CO, NH_3, CH_4 and C_3H_8 and oxidation of CO, CH_4 and C_3H_8 have been investigated. CO oxidation was carried out in the presence of O_2. Typical TPR profiles of reactants and products for $CO + O_2$ reaction are shown in figure 4. CO oxidation by O_2 starts at 170 °C and complete CO oxidation occurs below 350 °C. In contrast, complete CO to CO_2 conversion occurs below 200 °C over thermally treated Au/CeO_2 (figure 4(b)).

Complete oxidation of CH_4 over as-prepared 1% Au/CeO_2 occurs below 600 °C, whereas complete C_3H_8 oxidation to CO_2 and H_2O occurs below 425 °C. The complete CH_4 and C_3H_8 oxidation occur at 530 and 360 °C respectively over the heat-treated 1% Au/CeO_2.

Similarly NO and CO in 1:1 ratio were passed over the as-prepared Au/CeO_2 catalyst. NO reduction by CO starts at 200 °C and complete NO conversion to N_2 occurs below 450 °C. On the other hand, complete NO conversion over the heat-treated sample occurs below 350 °C.

NO reduction by NH_3 over this catalyst was also carried out with $NO + NH_3$ in 6:4 ratio. Complete conversion of NO is observed over as-prepared sample below 675 °C, whereas it occurs at 375 °C on heat-treated sample. Similarly complete NO reduction by CH_4 and C_3H_8 over thermally treated catalyst occurs at 675 and 585 °C respectively.

The temperatures of 100% conversion of NO, CO, CH_4 and C_3H_8 for all the reactions over the as-prepared and thermally-treated 1% Au/CeO_2 catalysts are summarized in table 1. Results on the same reaction over 1% Au/Al_2O_3 are given for comparison in the table. The respective reactions over 1% Au/Al_2O_3 catalyst occur at higher temperatures. Among the catalysts, heat-treated Au/CeO_2 shows the highest catalytic activity. It is important to note that all the reactions occur at much higher temperatures over a pure CeO_2 catalyst [33].

Table 1
100% conversion temperatures (°C) of NO, CO and hydrocarbons for reactions over 1% Au/CeO_2, heated 1% Au/CeO_2 and 1% Au/Al_2O_3 catalysts

Reactions	1% Au/CeO_2	Heated 1%Au/CeO_2	1% Au/Al_2O_3
$CO + O_2$	350	200	500
$CH_4 + O_2$	600	530	700
$C_3H_8 + O_2$	425	360	700
$NO + CO$	450	350	725
$NO + NH_3$	675	375	740
$NO + CH_4$	735	675	>750
$NO + C_3H_8$	650	585	>750

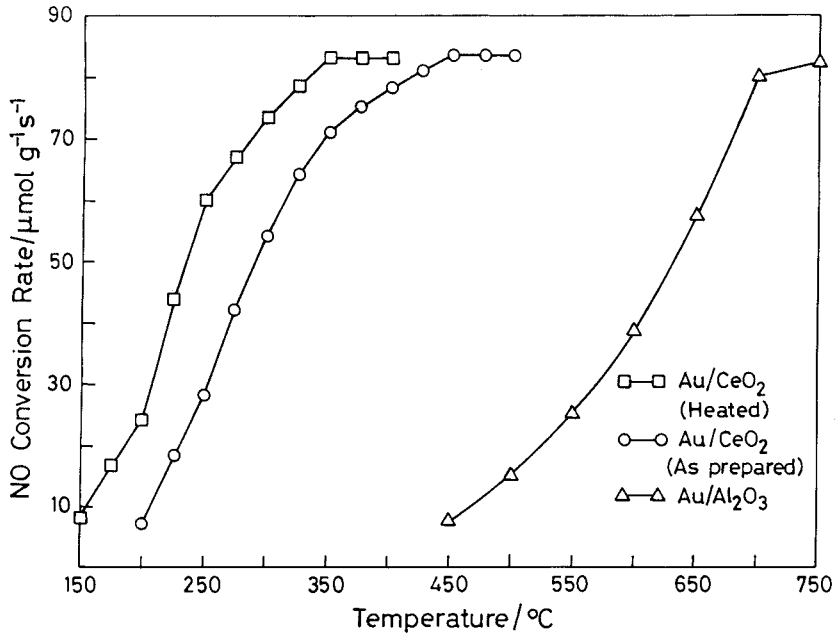

Figure 5. Rate of NO conversion as a function of temperature over as-prepared and heat-treated 1% Au/CeO_2 and 1% Au/Al_2O_3.

3.4. Kinetics

The rate of the reaction is calculated by the equation [41]

$$\text{Rate} = \frac{FX}{\nu W} \tag{2}$$

where F is the inlet molar flow rate of NO or CO, X is the fractional NO or CO conversion at a particular temperature, ν is the stoichiometric coefficient of NO or CO and W is the weight of the catalyst. The rate is expressed in $\mu\text{mol g}^{-1}\text{ s}^{-1}$. A comparison of NO conversion rates at different temperatures for NO + CO reaction over all the catalysts is shown in figure 5. The turnover frequencies (TOF) of reactions at different temperatures have been calculated by dividing the rate by the active site concentration and it is expressed in s^{-1}. The rate and TOF data of NO + CO and $C_3H_8 + O_2$ reactions over as-prepared and heated 1% Au/CeO_2 are given in table 2. TOF of NO + CO reaction over heat-treated and as-prepared 1% Au/CeO_2 are 0.94 and 1.28 s^{-1} respectively at 300 °C.

Table 2
Rate ($\mu\text{mol g}^{-1}\text{ s}^{-1}$) and TOF ($s^{-1}$) data of NO + CO and $C_3H_8 + O_2$ reactions over as-prepared as well as heated Au/CeO_2

Catalyst	NO + CO		$C_3H_8 + O_2$	
	Rate	TOF	Rate	TOF
As-prepared	28.3 (250 °C)	0.49 (250 °C)	16.7 (350 °C)	0.29 (350 °C)
	54.0 (300 °C)	0.94 (300 °C)	50.0 (375 °C)	0.87 (375 °C)
Heated	60.0 (250 °C)	1.0 (250 °C)	103.3 (350 °C)	1.79 (350 °C)
	73.3 (300 °C)	1.28 (300 °C)	166.7 (375 °C)	2.90 (375 °C)

From the conversion data and the reaction conditions, rate constants have been calculated at different temperatures. For a packed bed tubular reactor the first-order rate constant k with respect to CO for

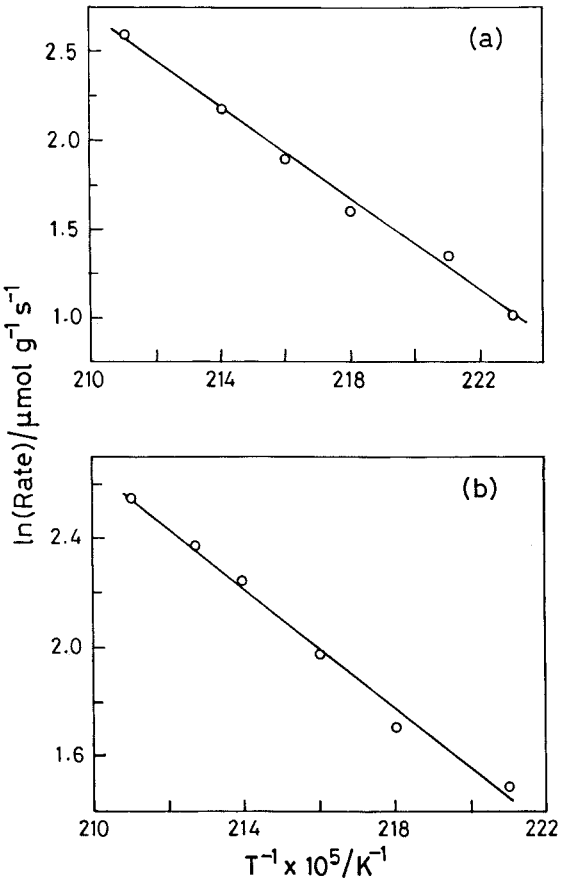

Figure 6. Arrhenius plots of $CO + O_2$ reaction over (a) as-prepared 1% Au/CeO_2 and (b) heat-treated 1% Au/CeO_2.

$CO + O_2$ reaction is given by [42,43]

$$k(\mathrm{cm^3\,g^{-3}\,s^{-1}}) = -\frac{F}{[\mathrm{CO}]W}\ln(1-X) \qquad (3)$$

where F is the inlet molar flow rate of CO, [CO] is the inlet molar concentration of CO, W is the weight of the catalyst and X is the fractional CO conversion at a particular temperature. Rate constants for $CO + O_2$ over as-prepared 1% Au/CeO_2 are 2.71×10^3 and $4.9 \times 10^3\,\mathrm{cm^3\,g^{-1}\,s^{-1}}$ at 250 °C and 300 °C respectively.

The activation energies (E_a) are calculated from Arrhenius plots of ln(Rate) *versus* $1/T$. Here CO_2 formation rates have been taken into account for the calculation in the temperature range 175–210 °C. Activation energy for $CO + O_2$ over the as-prepared sample is $106\,\mathrm{kJ\,mol^{-1}}$, whereas that on the heated sample is $90\,\mathrm{kJ\,mol^{-1}}$. Typical Arrhenius plots are shown in figure 6.

4. Discussion

Gold dispersed on conventional supports such as SiO_2 or Al_2O_3 is not quite active, whereas transition metal oxide supported gold catalysts exhibit high and unusual activity towards different kinds of reactions, especially CO oxidation at relatively low temperature. In particular, Au/Al_2O_3, Au/TiO_2 and Au/Co_3O_4 are effective catalysts for CO oxidation. But there are several opinions regarding the mechanism associated with the high activity of these catalysts. Minicò *et al.* [28] have shown by FTIR study that Au^+ is more active in CO oxidation and less stable than Au^0. Boccuzzi and Chiorino [44] have recently reported that CO is molecularly adsorbed on top of the Au sites and reacts with the O_2.

In the present study, Au nano particles as well as oxidized Au species prepared by a single step combustion provide the active sites for the catalytic reactions. Here CO, NO and hydrocarbons are adsorbed on fine Au particles as well as Au^{3+} species. Interestingly, heat-treated Au/CeO_2 shows better catalytic activity compared with as-prepared catalyst. Even the temperature for $CO + O_2$ reaction is comparable with the same reaction over 1% Pt/CeO_2 [45]. In the as-prepared 1% Au/CeO_2, about 30% of Au is present in the +3 oxidation state and the rest are seen as nano Au particles. The color of the as-prepared 1% Au/CeO_2 is light violet. XRD as well as TEM studies clearly show the presence of 5–10 nm Au particles. In fact, 2% Au/CeO_2 shows more Au particles in TEM and also the Au(111) peak in XRD is more intense. Accordingly, the color of 2% Au/CeO_2 is intense violet, indicating the presence of more Au metal particles. On the other hand, Au/Al_2O_3 where Au is present only as fine Au metal particles is chocolate brown in color, suggesting Au fine particles dispersed on Al_2O_3 [34]. On heating 1% Au/CeO_2 to 800 °C for 100 h in air, the color changes from light violet to light gray and formation of Au(III) oxide species may take place. XPS study shows the increase in concentration of Au^{3+} in the heat-treated sample. It is important to note that we do not see any indication of Au^{1+} state in the as-prepared as well as the heat-treated samples from the XPS study. Further, TEM of heat-treated Au/CeO_2 does not show many Au particles. CeO_2 particle surfaces are flat and clean. We therefore conclude that heat-treated 1% Au/CeO_2 contains more Au^{3+} ions. Again, surface concentration of Au increases from 10 to 16% on heating. Indeed, total concentration of Au(4f) peaks in the XPS spectrum increases on heat-treatment. All these observations suggest the interaction of Au particles with CeO_2. The ionic radii of Ce^{4+} and Au^{3+} are 0.97 and 0.85 Å respectively [46]. Therefore, there is a possibility of stabilization of Au^{3+} ion in the form of a solid solution of type $Ce_{1-x}Au_xO_{2-\delta}$ on the surface of as-prepared as well as heat-treated samples. The amount of solid solution could be more in heat-treated sample. However, Pt^{2+} and Au^{3+} are isoelectronic having $5d^8$ electronic configuration. Therefore, heat-treated 1% Au/CeO_2 containing more Au^{3+} sites should resemble the catalytic behavior of 1% Pt/CeO_2. Especially for $CO + O_2$ reaction, Au^{3+}/CeO_2 shows Pt^{2+}/CeO_2 like behavior. However, CH_4 oxidation and NO reduction by CH_4 and C_3H_8 over the heat-treated sample occur at higher temperatures in relation to Pt/CeO_2. From figure 4 and table 1 it is clear that CO to CO_2 and other reactions carried out here occur at lower temperatures over heat-treated Au/CeO_2 compared with as-prepared Au/CeO_2 and Au/Al_2O_3. Increase in the Au^{3+} ion concentration on CeO_2 surface is the only change that occurs on heat treatment. Therefore, we attribute the decrease in reaction temperature, increase in the rate and decrease in the activation energy to the presence of more Au^{3+} ions on CeO_2 along with small Au particles.

5. Conclusions

The salient features of this investigation are:

1. The combustion method is a new technique for the preparation of Au/CeO_2 catalyst.
2. Au is dispersed on CeO_2 surface in metallic as well as ionic form.
3. On heat-treatment concentration of Au^{3+} species increases.
4. Both Au^0 and Au^{3+} species act as catalytic sites in Au/CeO_2 catalyst.
5. All the reactions over heat-treated 1% Au/CeO_2 occur at lower temperatures compared with as-prepared 1% Au/CeO_2 and 1% Au/Al_2O_3.
6. Rate and TOF of heat-treated 1% Au/CeO_2 are higher compared with the as-prepared sample.

Acknowledgment

P. Bera is grateful to the Council of Scientific and Industrial Research (CSIR), Government of India, for the award a research fellowship. We are grateful to Professor K.C. Patil for useful discussion. The Department of Atomic Energy (DAE) and Department of Science and Technology (DST), Government of India, are gratefully acknowledged for funding this research. Thanks are due to Dr. G. N. Subbanna for recording TEM.

References

[1] M. Haruta, N. Yamada, T. Kobayashi and S. Iijima, J. Catal. 115 (1989) 301.
[2] M. Haruta, S. Tsubota, T. Kobayashi, H. Kageyama, M. J. Genet and B. Delmon, J. Catal. 144 (1993) 175.
[3] F. Boccuzzi, A. Chiorino, S. Tsubota and M. Haruta, Catal. Lett. 29 (1994) 225.
[4] W. S. Epling, G. B. Hoflund, J. F. Weaver, S. Tsubota and M. Haruta, J. Phys. Chem. 100 (1996) 9929.
[5] A. K. Tripathi, V. S. Kamble and N. M. Gupta, J. Catal. 187 (1999) 332.
[6] M. A. Bollinger and M. A. Vannice, Appl. Catal. B 8 (1996) 417.
[7] M. A. P. Dekkers, M. J. Lippits and B. E. Nieuwenhuys, Catal. Lett. 56 (1998) 195.
[8] J.-D. Grunwaldt, M. Maciejewski, O. S. Becker, P. Fabrizioli and A. Baiker, J. Catal. 186 (1999) 458.
[9] S. D. Lin, M. Bollinger and M. A. Vannice, Catal. Lett. 17 (1993) 245.
[10] F. Boccuzzi, G. Cerrato, F. Pinna and G. Strukul, J. Phys. Chem. B 102 (1998) 5733.
[11] M. M. Schubert, S. Hackenberg, A. C. van Veen, M. Muhler, V. Plzak and R. J. Behm, J. Catal. 197 (2001) 113.
[12] Y.-J. Chen and C.-T. Yeh, J. Catal. 200 (2001) 59.
[13] R. A. Koeppel, A. Baiker, C. Schild and A. Wokaun, J. Chem. Soc. Faraday Trans. 87 (1991) 2821.
[14] S. Lin and M. A. Vannice, Catal. Lett. 10 (1991) 47.
[15] H. Sakurai, S. Tsubota and M. Haruta, Appl. Catal. A 102 (1993) 125.
[16] H. Sakurai and M. Haruta, Appl. Catal. A 127 (1995) 93.
[17] D. Andreeva, V. Idakiev, T. Tabakova and A. Andreev, J. Catal. 158 (1996) 354.
[18] R. D. Waters, J. J. Weimer and J. E. Smith, Catal. Lett. 30 (1995) 181.
[19] K. Blick, T. D. Mitrelias, J. S. J. Hargreaves, G. J. Hutchings, R. W. Joyner, C. J. Kiely and F. E. Wagner, Catal. Lett. 50 (1998) 211.
[20] A. Ueda, T. Oshima and M. Haruta, Appl. Catal. B 12 (1997) 81.
[21] S. Galvagno and G. Parravano, J. Catal. 55 (1978) 178.
[22] J. Y. Lee and J. Schwank, J. Catal. 102 (1986) 207.
[23] S. K. Tanielyan and R. L. Augustine, Appl. Catal. A 85 (1992) 73.
[24] M. Valden, X. Lai and D. W. Goodman, Science 281 (1998) 1647.
[25] J.-D. Grunwaldt, C. Kiener, C. Wögerbauer and A. Baiker, J. Catal. 181 (1999) 223.
[26] R. J. H. Grisel, P. J. Kooyman and B. E. Nieuwenhuys, J. Catal. 191 (2000) 430.
[27] G. C. Bond and D. T. Thompson, Catal. Rev.-Sci. Eng. 41 (1999) 319.
[28] G. C. Bond and D. T. Thompson, Gold Bull. 33 (2000) 41.
[29] S. Minicò, S. Scirè, C. Crisafulli, A. M. Visco and S. Galvagno, Catal. Lett. 47 (1997) 273.
[30] T. M. Salama, T. Shido, H. Minagawa and M. Ichikawa, J. Catal. 152 (1995) 322.
[31] E. A. Shaw, A. P. Walker, T. Rayment and R. M. Lambert, J. Catal. 134 (1992) 747.
[32] W. Liu and M. Flytzani-Stephanopoulos, J. Catal. 153 (1995) 317.
[33] P. Bera, S. T. Aruna, K. C. Patil and M. S. Hegde, J. Catal. 186 (1999) 36.
[34] P. Bera, K. C. Patil, V. Jayaram, M. S. Hegde and G. N. Subbanna, J. Mater. Chem. 9 (1999) 1801.
[35] P. Bera, K. C. Patil and M. S. Hegde, Phys. Chem. Chem. Phys. 2 (2000) 373.
[36] P. Bera, K. C. Patil and M. S. Hegde, Phys. Chem. Chem. Phys. 2 (2000) 3715.
[37] A. M. Visco, F. Neri, G. Neri, A. Donato, C. Milone and S. Galvagno, Phys. Chem. Chem. Phys. 1 (1999) 2869.
[38] T. J. Zhou, G. J. Mains and J. M. White, J. Phys. Chem. 91 (1987) 5931.
[39] J. H. Scofield, J. Electron Spectrosc. Relat. Phenom. 8 (1976) 129.
[40] D. R. Penn, J. Electron Spectrosc. Relat. Phenom. 29 (1976) 9.
[41] R. L. Burwell, Jr., Pure Appl. Chem. 46 (1976) 71.
[42] J. M. Thomas and W. J. Thomas, in: *Introduction to the Principles of Heterogeneous Catalysis* (Academic Press, London, 1967) ch. 9, p. 451.
[43] F. Kapteijn and J. A. Moulijn, in: *Handbook of Heterogeneous Catalysis*, Vol. 3, eds. G. Ertl, H. Knözinger and J. Weitkamp (VCH, Weinheim, 1997) p. 1359.
[44] F. Boccuzzi and A. Chiorino, J. Phys. Chem. B 104 (2000) 5414.
[45] P. Bera, K. C. Patil, V. Jayaram, G. N. Subbanna and M. S. Hegde, J. Catal. 196 (2000) 293.
[46] R. D. Shannon, Acta Crystallog. A 32 (1976) 751.